Magnetoelastic properties of antiferromagnetically coupled magnetic composite media

Juan J. Valencia-Cardona and Perry H. Leo*
Department of Aerospace Engineering and Mechanics, University of Minnesota, Minneapolis, Minnesota 55455, USA
(Received 19 July 2016; published 24 August 2016)

We study the magnetic response of a ferromagnetic bilayer with antiferromagnetic coupling, where the layers experience magnetostrictive strains and epitaxial misfit strains. These strains cause the layers to stretch and bend as the magnetic spins of the layers rotate, resulting in elastic energy that adds to the magnetic energy of the system. The magnetic and elastic energies are computed as a function of spin direction in each layer for a given set of material and geometric parameters. By finding the rotations that minimize the total energy, we compute magnetic hysteresis loops for different combinations of magnetic and elastic parameters. The elastic contribution is reflected in the transitions at the corners of the hysteresis curves as well as in the coercive field of the main loop. The details of the elastic contribution depend in a complicated way on the magnetostriction of the layers, the epitaxial strain, the magnetic anisotropies, and the system geometry.

DOI: 10.1103/PhysRevB.94.054425

I. INTRODUCTION

Thin films consisting of ferromagnetic layers have been studied extensively over the last few decades, owing to their applications as microactuators, micromotors, magnetic sensors, spin-transfer nano-oscillators, magnetoresistive random-access memory (MRAMs), and spin valves, among others [1–9]. Ferromagnetic layers can exhibit antiferromagnetic coupling, for example by including an appropriate nonmagnetic layer between the ferromagnetic layers. Adjusting the nonmagnetic layer thickness affects the strength of the exchange interaction between the ferromagnetic layers, while changing the ferromagnetic layer thickness varies the magnetic anisotropy [5,6,10–12]. Examples of multilayered ferromagnetic systems with antiferromagnetic coupling include media multilayers such as Fe/Cr, Co/Cu, Fe/Cu, and Co/Ru [10–12]. There has also been significant work on "exchange springs," where magnetostrictive strains of the ferromagnetic layers are used to vary the exchange energy by changing layer thicknesses. Examples include TbFe/TbFe, $TbFe_2$/Fe, and TbFe/FeCuNbSiB multilayers [13–17]. The magnetostrictive behavior is often explored by measuring the curvature of the multilayer [15,16] or by inspecting magnetization curve behavior, e.g., changes in the coercive field and squareness of the hysteresis loops [8,18,19].

While ferromagnetic mutilayers have interesting magnetic and magnetoelastic properties, there has been relatively little work addressing the coupling between the two processes. Shima *et al.* have measured magnetization curves in antiferromagnetically coupled bilayers, and have also measured the magnetoelastic coupling coefficient as a function of applied field [15,16]. Their results suggest some correlation between the magnetostrictive strains and the rotation of the layer spins, where strain levels change as the relative thickness of the layers change. In a somewhat different setting, Pertsev and Kohlstedt have shown that in ferromagnetic multilayers on a ferroelectric substrate, elastic energy can be used to trigger the switching of magnetic moments under moderate electric fields [20].

In this paper, we study the magnetic response of a ferromagnetic bilayer with antiferromagnetic coupling, where the layers experience magnetostrictive strains as well as epitaxial misfit strains. Our goal is to identify how and where elasticity can alter magnetic hysteresis curves of such systems, and to characterize the parameter space where such effects can be observed.

We accomplish this by computing the magnetic and elastic energies as functions of the layer spin rotations and material parameters. The magnetic energy of the multilayer system is taken following Dantas *et al.* [21]; see also [6,10,22–30]. The elastic energy of the system is found by using a model similar to that of Hsueh *et al.* [31], although in our case strains arise from a magnetostrictive response to an external magnetic field, rather than from a change in temperature. We use a numerical minimization algorithm to find the layer spin rotations that minimize the magnetic plus elastic energy, which allows us to study the effects of magnetic, mechanical, and system properties on the magnetic response. Specifically, we compute hysteresis loops for different values of system parameters. The hysteresis curves without elastic coupling are in qualitative agreement with previous results; see [5,6,11,12,15]. The elastic contribution affects the transitions at the corners of the hysteresis curves as well as the coercive field of the main loop.

In the following, we detail the magnetic and elastic energies used in the model. We briefly describe the computation of the magnetic response, and we present and discuss the results.

II. MODEL DEVELOPMENT

A two-layer ferromagnetic film with antiferromagnetic coupling is studied; see Fig. 1. Following Dantas *et al.* [21,32] (see also [22–25,27–29]), we consider two ferromagnetic layers, each with a single spin in the plane of the film (the x-y plane). Both layers have uniaxial symmetry, with the easy axis of magnetization coinciding with the x axis. The external magnetic field H is applied along the x axis. The layers have thicknesses t_1 and t_2 so that the thickness ratio

$$\beta = \frac{t_1}{t_2}. \tag{1}$$

*phleo@umn.edu

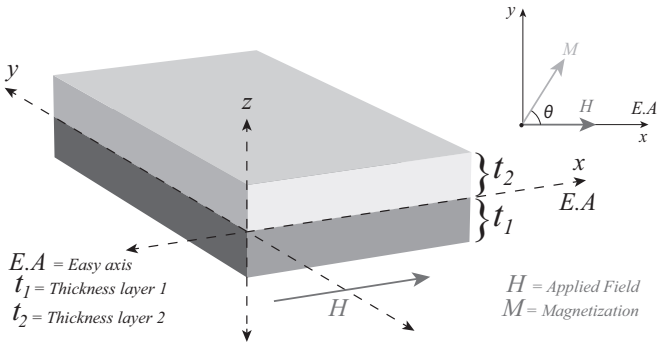

FIG. 1. Multilayer system schematic. Magnetization M and applied field H position with respect to the easy axis.

We take $t_1 \leqslant t_2$ so that $0 < \beta \leqslant 1$.

The magnetic energy per unit area of the system is taken as

$$E_{\text{mag}} = -HM_s\beta\cos(\theta_1) - HM_s\cos(\theta_2) + j_{2:1}\beta\cos(\theta_2-\theta_1) - \frac{k_1}{2}\beta^2\cos^2(\theta_1) - \frac{k_2}{2}\cos^2(\theta_2). \tag{2}$$

Here, θ_1 and θ_2 are the angles that the in-plane magnetization vector M makes with respect to the easy axis (EA) (see Fig. 1). Also, M_s is the constant saturation magnetization, taken to be the same in both layers. Hence, $M_s\cos(\theta)$ gives the component of the magnetization in the x direction. The values k_1 and k_2 are the anisotropy constants of the layers, and $j_{2:1}$ is the *negative* of the exchange integral, as discussed below.

The first two terms in Eq. (2) describe the Zeeman energy of the layers [33–35]. The Zeeman energy favors the magnetization in the direction of the applied field. The third term is the exchange energy between layers, which favors either parallel (ferromagnetic) or antiparallel (antiferromagnetic) coupling of the spins. The difference between the two cases depends on the sign of the exchange integral, $J = -j_{2:1}$. The exchange integral is negative for antiferromagnetic coupling [21,33] (hence our $j_{2:1}$ is positive) and so favors antiparallel spins. We define a positive exchange coefficient in order to simplify normalization of the energy. The last two terms of Eq. (2) are the anisotropy energy contributions of the system, where the anisotropy factors k_1 and k_2 determine the energy cost of moving the magnetization away from the easy axis. Equation (2) is valid for single-domain ferromagnetic layers, which are reversing their magnetization coherently.

The elastic energy of the bilayer system results from the fact that when an external field is applied parallel (or antiparallel) to the easy axis, the individual layers will want to expand or contract depending on their magnetostrictive properties. In general, and assuming the layers are well bonded, any differential expansion/contraction will cause the multilayered system to expand/contract and bend. This leads to residual stresses in the individual layers, and hence to an elastic energy.

We derive this elastic energy as follows [31]. Noting that the z axis is normal to the layers, we set $z = 0$ at the junction between the layers. The strain distribution of the system owing to expansion/contraction and bending is taken to be linear in z,

$$\epsilon_0(z) = \epsilon_c + \frac{t_b - z}{r}, \tag{3}$$

where ϵ_c defines the uniform part of the strain and $\frac{t_b-z}{r}$ describes the bending, with t_b and r^{-1} as the bending axis and radius of curvature, respectively. The bending direction of the film (concave or convex) depends on the sign of the radius of curvature r^{-1}.

The residual stress in each layer is proportional to an "elastic" strain, given by the difference between the total strain from Eq. (3) and the "stress-free" or misfit strain of each layer. We take the misfit strain to be the sum of an epitaxial strain and a magnetostrictive strain, where the epitaxial strain arises from the different lattice parameters of the two layers in the absence of a magnetic field. That is, the elastic strain in each layer is given by

$$\epsilon_1(z) = \epsilon_0(z) - \epsilon^{T_1} - \lambda_1\cos^2(\theta_1) \tag{4}$$

and

$$\epsilon_2(z) = \epsilon_0(z) - \epsilon^{T_2} - \lambda_2\cos^2(\theta_2). \tag{5}$$

Here, ϵ^{T_1} and ϵ^{T_2} are the stress-free strains of the two layers relative to some common reference state and in the absence of any magnetostriction. We take $\epsilon^T = \epsilon^{T_1} - \epsilon^{T_2}$ as the epitaxial strain between the two layers; this is equivalent to taking the common reference state to be the unstrained lattice of layer 2. The coefficients λ_1 and λ_2 are magnetic expansion coefficients and give the magnetostrictive strain when the magnetic moment is aligned along the easy axis, so θ is 0 or π. Hence the projections of the magnetic moment onto the easy axis is proportional to $\cos(\theta_i)$ $(i = 1,2)$ (see Fig. 1). We use $\cos^2(\theta)$ in Eqs. (4) and (5) to reflect that the magnetostrictive strain is the same for magnetization angles $\theta = 0$ and π.

Assuming the layers are linear elastic, the stresses in the two layers are simply proportional to the elastic strain, so

$$\sigma_1(z) = Y_1\epsilon_1(z) \quad \text{for} \quad -t_1 \leqslant z \leqslant 0, \tag{6}$$

and

$$\sigma_2(z) = Y_2\epsilon_2(z) \quad \text{for} \quad 0 \leqslant z \leqslant t_2, \tag{7}$$

where Y_1 and Y_2 denote the Young's modulus of each layer.

In order to obtain the unknown parameters ϵ_c, t_b, and r^{-1}, we specify that the resultant forces and moments on the bilayer system must vanish. We set the resultant force in the system owing to uniform strain and bending to zero,

$$Y_1[\epsilon_c - \epsilon^T - \lambda_1\cos^2(\theta_1)]t_1 + Y_2[\epsilon_c - \lambda_2\cos^2(\theta_2)]t_2 = 0 \tag{8}$$

and

$$\int_{-t_1}^{0} \frac{Y_1(z-t_b)}{r}dz + \int_{0}^{t_2} \frac{Y_2(z-t_b)}{r}dz = 0. \tag{9}$$

We also set the resultant moment on the bilayer about $z = t_b$ to zero,

$$\int_{-t_1}^{0} \sigma_1(z-t_b)dz + \int_{0}^{t_2} \sigma_2(z-t_b)dz = 0. \tag{10}$$

Solving Eqs. (8)–(10) yields

$$\epsilon_c = \frac{\beta\epsilon^T + \beta\lambda_1\cos^2(\theta_1) + \lambda_2\cos^2(\theta_2)}{1+\beta}, \tag{11}$$

$$\frac{1}{r} = -\frac{1}{t_2(1+\beta)^3} \times 3\beta\{2\epsilon^T + (\lambda_1 - \lambda_2) + [\lambda_1\cos(2\theta_1) - \lambda_2\cos(2\theta_2)]\} \tag{12}$$

and

$$t_b = \frac{t_2(1-\beta)}{2}, \tag{13}$$

where the thickness ratio β is defined in Eq. (1). Note that the uniform strain ϵ_c and the bending curvature r^{-1} depend on the directions of the magnetic moments through θ_1 and θ_2, while the bending axis t_b depends only on the layer thicknesses.

In our subsequent analysis, we simplify these results by taking the elastic moduli to be equal, so $Y_1 = Y_2 = Y$. We compute the elastic energy per unit area as [36]

$$E_{\text{elas}} = \frac{1}{2}\int_{-t_1}^{0}(\sigma_1\epsilon_1)dz + \frac{1}{2}\int_{0}^{t_2}(\sigma_2\epsilon_2)dz. \tag{14}$$

After some algebra, we find that the elastic energy of the bilayer system is

$$E_{\text{elas}} = \tfrac{1}{8}Yt_2\psi\{2\epsilon^T + (\lambda_1 - \lambda_2) + [\lambda_1\cos(2\theta_1) - \lambda_2\cos(2\theta_2)]\}^2, \tag{15}$$

where $\psi = \beta[1+\beta(\beta-1)]/(1+\beta)^3$ is a constant that depends on the thickness ratio β.

As mentioned in Sec. I, antiferromagnetic coupling is often achieved by using a thin nonmagnetic layer separating the ferromagnetic layers. While it is straightforward to include extra layers in the elasticity calculation, we do not. Our primary reason for this is that including the nonmagnetic layer adds to the parameter space and makes it more difficult to interpret the results. Moreover, the calculations we have done (albeit not in the full parameter space) indicate that the nonmagnetic layer does not significantly affect the results until its thickness is roughly the same order as the ferromagnetic layers.

We have also considered a magnetoelastic energy that arises from the dependence of the magnetization on elastic strains [37–39]. However, because the strains in our case arise from magnetostriction, this additional energy is small compared to the elastic energy from the residual layer stresses owing to magnetostriction, and so we do not include it here.

Total energy and normalization

The total energy of the system is the sum of the magnetic and elastic energies from Eqs. (2) and (15). For consistency, and following [21], we normalize both the magnetic and elastic energies using the exchange energy $j_{2:1}$. This yields a normalized total energy,

$$E_{\text{total}} = \frac{\beta}{2}\cos(\theta_2 - \theta_1) - \beta^2\frac{\alpha_1}{2}\cos^2(\theta_1) - \frac{\alpha_2}{2}\cos^2(\theta_2) - h\beta\cos(\theta_1) - h\cos(\theta_2) + \frac{1}{16}Y_{\text{mod}}\psi\{2\epsilon^T + (\lambda_1 - \lambda_2) + [\lambda_1\cos(2\theta_1) - \lambda_2\cos(2\theta_2)]\}^2, \tag{16}$$

where $\alpha_1 = k_1/(2j_{2:1})$ and $\alpha_2 = k_2/(2j_{2:1})$ are the normalized anisotropies, $H_E = (2j_{2:1})/M_s$ is the exchange field, $h = H/H_E$ is the normalized applied field, and $Y_{\text{mod}} = Y/j_{2:1}$ is the normalized modulus of elasticity.

We use magnetic hysteresis loops as an observable for the different mechanical effects on the magnetic response. In order to find the M vs h curves, the average magnetization of the system in the direction of the easy axis is defined as

$$\overline{M} = \frac{t_1M_1 + t_2M_2}{t_1 + t_2}, \tag{17}$$

where $M_{(1,2)} = M_s\cos(\theta_{(1,2)})$. Hence,

$$\frac{\overline{M}}{M_s} = \frac{\beta\cos[\theta_1(h)] + \cos[\theta_2(h)]}{1+\beta}. \tag{18}$$

In the following analysis, we set the material properties of the two layers through the parameters α_1, α_2, Y_{mod}, ϵ^T, λ_1, and λ_2. We set the geometry through the thickness ratio β. Once these properties are specified, the energy (16) may be considered as a function of the magnetization angles θ_1 and θ_2, parameterized by the applied magnetic field h. We study the magnetic behavior of the system by finding the critical angles θ_{c1} and θ_{c2} that minimize the energy for a given set of parameters and as a function of the normalized applied field h. These critical angles are then used to construct the magnetization curves via Eq. (18).

The critical angles are found by using an energy-minimizing algorithm. This algorithm was developed by combining a pseudo-arc-length algorithm and a steepest descent energy minima tracking technique [40,41]. The pseudo-arc-length algorithm tracks equilibrium points of the energy that are not necessarily stable, in which case the steepest descent is activated and finds the closest stable point in the neighborhood of the unstable equilibrium point. See the Supplemental Material [42] for details.

III. RESULTS

All results are generated by using material parameters consistent with the experimental values shown in Table I. We first consider the magnetic response in the absence of elastic energy by considering two different pairs of anisotropies at several different thickness ratios. These results are analogous to those of Dantas *et al.* for a two-layer system [21]. We then consider how elasticity affects the baseline magnetization curves by choosing a range of values for the epitaxial strain ϵ^T and the magnetic expansion coefficients λ_1 and λ_2.

TABLE I. List of parameters involved in calculations.

Parameter	Symbol	Magnitude
Magnetization[a]	M_s	$\sim 10^6$ A m^{-1}
Magnetic field[b]	H	~ 1 T
Exchange[c]	j	$\sim 10^6$ J m^{-3}
Anisotropy[d]	k	$\sim 10^5$ J m^{-3}
Stress[e]	σ	[Pa]
Young's modulus[f]	Y	~ 200 GPa
Strain[g]	ϵ	$\sim 10^{-3}$
Thickness ratio[h]	β	0.2 to 1
Normalized modulus	Y_{mod}	30 000
Magnetoelastic coefficient[i]	λ	$\sim 10^{-3}$
Normalized anisotropy[j]	α	0.15 and 0.3
Normalized field	h	-1 to 1

[a]Consistent with [12].
[b]Field required for saturation depends on the sample.
[c]Consistent with [10,11,23].
[d]Consistent with [5,11].
[e]Varies with strain and Young's modulus.
[f]Roughly that of metals such as Fe and Ni.
[g]Typical value for epitaxial strain.
[h]As in [21].
[i]Consistent with [13,15,16].
[j]Consistent with [12,21,43].

A. No elasticity, $\alpha_1 = 0.15$ and $\alpha_2 = 0.3$

When $\alpha_1 = 0.15$ and $\alpha_2 = 0.3$, layer 1 has a smaller magnetic anisotropy energy than layer 2. Moreover, since $\beta = t_1/t_2 \leqslant 1$, layer 1 is the thinner layer. Hence both the anisotropy and thickness ratio have values such that it should be easier to rotate the magnetization of layer 1 compared to layer 2. Figure 2 shows the magnetic hysteresis loop for different values of β. In all hysteresis curves, increasing field is shown as a solid line, while decreasing field is shown as a dashed line. Regions with identical response to increasing and decreasing fields are also seen as a solid line.

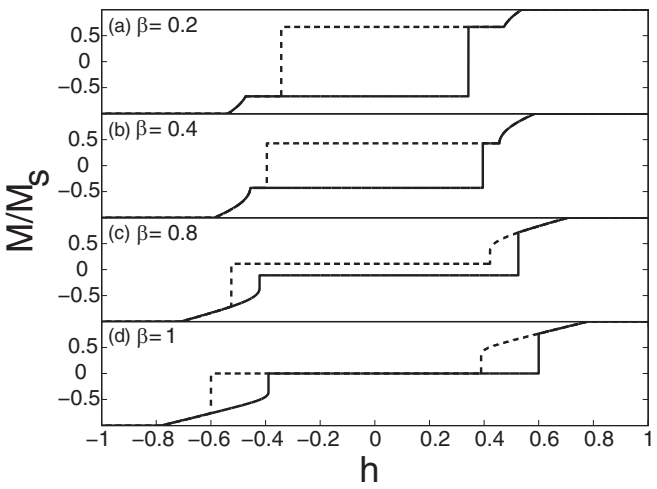

FIG. 2. Magnetic hysteresis curves are shown for different values of the layer thickness ratio β when $\alpha_1 = 0.15$ and $\alpha_2 = 0.3$.

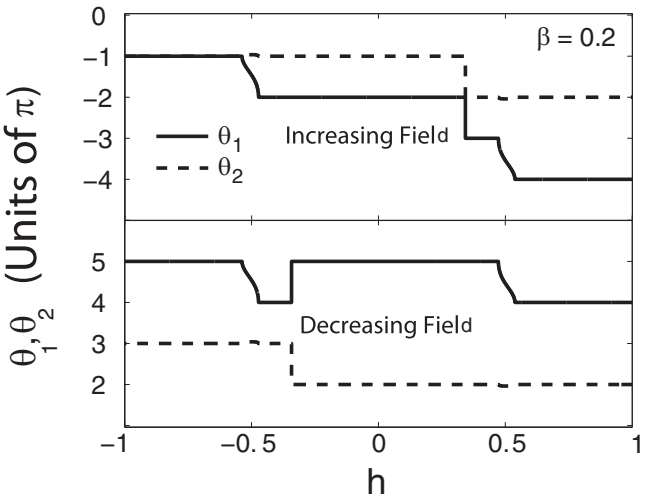

FIG. 3. The spin angles θ_1 and θ_2 are shown for the case corresponding to $\beta = 0.2$, $\alpha_1 = 0.15$, and $\alpha_2 = 0.3$. The top figure shows the angles on increasing the external magnetic field from -1, while the lower curve shows the angles on decreasing the field from $+1$. The actual results from the minimization algorithm are shown, though θ_1 and θ_2 are 2π periodic.

Consider the case $\beta = 0.2$ in Fig. 2(a). The spin rotations θ_1 and θ_2 associated with this hysteresis curve are shown in Fig. 3, and determine the magnetic response through Eq. (18). Also, while we show the actual results from the minimization algorithm in Fig. 3, we report values of θ_1 and θ_2 between 0 and 2π as the energy of Eq. (16) is 2π periodic in θ_1 and θ_2.

When the applied field $h = -1$, the system is fully saturated ($\theta_1 = \theta_2 = \pi$). Upon increasing the field, the system stays saturated until $h \approx -0.54$, at which point layer 1 rotates to $\theta_1 = 0$. This behavior is known as a spin floplike transition and typically occurs for a ferromagnetic to antiferromagnetic (and vice versa) transition [21,33]. This antiferromagnetically coupled state persists until $h \approx 0.35$, when the direction of moments reverse so that $\theta_1 = \pi$ and $\theta_2 = 0$. As h increases further, θ_1 eventually rotates to zero so both magnetizations are oriented in the direction of the applied field, i.e., the system saturates at $\theta_1 = \theta_2 = 0$. As h decreases from 1, the reverse process occurs, as shown by the decreasing field plot in Fig. 3.

The normalized remanent magnetization when $\beta = 0.2$ is 0.667. Since the remanent magnetization is measured as the half height between states $(\theta_1,\theta_2) = (0,\pi)$ and $(\pi,0)$, it is easily found to be

$$\frac{M_r}{M_s} = \frac{(1-\beta)}{(1+\beta)} \tag{19}$$

from Eq. (18).

As β increases, the width of the hysteresis curve (i.e., the coercive field) increases and the remanent magnetization decreases, consistent with Eq. (19). When $\beta = 0.4$ [Fig. 2(b)], the spin behavior is much like the $\beta = 0.2$ case. However, the initial rotation of the layer 1 spin as h increases from -1 (or decreases from 1) occurs more gradually, as expected from the fact that the relative thickness of layer 1 increases with β. At the same time, there is some corresponding rotation of the layer 2 spin. This trend continues as β increases, eventually leading

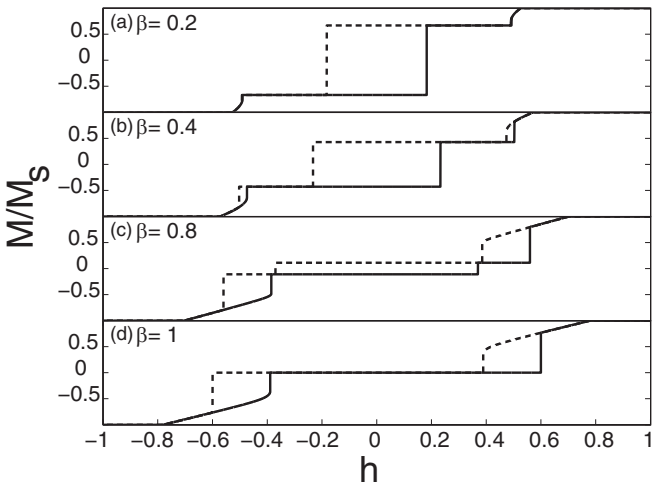

FIG. 4. Magnetic hysteresis curves are shown for different values of the layer thickness ratio β when $\alpha_1 = 0.3$ and $\alpha_2 = 0.15$.

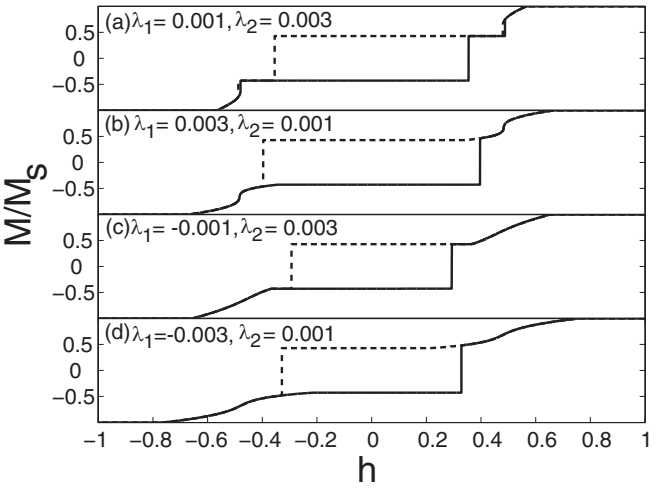

FIG. 5. Magnetic hysteresis curves are shown for different values of magnetostrictive strains λ_1 and λ_2, with epitaxial misfit $\epsilon^T = 0$ and thickness ratio $\beta = 0.4$. The magnetic anisotropies $\alpha_1 = 0.15$ and $\alpha_2 = 0.3$.

to a double-loop shape. At $\beta = 1$, the main hysteresis loop vanishes as expected from Eq. (19). This has been reported as the typical behavior of an antiferromagnetically coupled system [21,32] and should correspond to a first-order transition of the spin floplike state. On increasing field at $h = 0$, the system remains unmagnetized until $h \approx 0.6$, at which point the spins rotate towards saturation, which is achieved at $h \approx 0.8$.

B. No elasticity, $\alpha_1 = 0.3$ and $\alpha_2 = 0.15$

We now switch the magnetic anisotropies, so $\alpha_1 = 0.3$ and $\alpha_2 = 0.15$. Hence we expect a tradeoff between the anisotropy, which favors rotation of layer 2, and the thickness, which, since $t_1 \leqslant t_2$, favors rotation of layer 1.

Figure 4 shows the magnetic response for four different values of β. As it is now easier to rotate the magnetization of the thicker layer (layer 2), the coercive field of the main hysteresis loop is smaller than in the previous case. For example, when $\beta = 0.8$ and as h increases [Fig. 4(c)], the spin rotations flip from $(\theta_1,\theta_2) = (0,\pi)$ to $(\pi,0)$ at $h \approx 0.34$. This occurs because of the relatively low cost of rotating the spin of layer 2, while keeping the antiferromagnetic coupling between the layers. This is seen on the magnetization curve as a jump from the lower plateau to the upper plateau between $h \approx 0.34$ and $h \approx 0.53$, at which point θ_1 rotates toward zero. In contrast, in the $\beta = 0.8$ case shown in Fig. 2(c), there is no transition from the lower plateau to the upper plateau as h increases; (θ_1,θ_2) stays at $(0,\pi)$ until the field is strong enough to rotate θ_2 towards zero. Finally, when $\beta = 1$, the two layers have the same thickness, and so the cases $\alpha_1 = 0.3$, $\alpha_2 = 0.15$ and $\alpha_1 = 0.15$, $\alpha_2 = 0.3$ are identical.

C. Elastic effects

We now consider how elastic energy affects the magnetic response. As seen in Eq. (15), elastic energy depends on the magnetoelastic coefficients λ_1 and λ_2, the epitaxial strain ϵ^T, the normalized elastic modulus Y_{mod}, the thickness ratio β, and the magnetic rotations θ_1 and θ_2.

As before, we determine the magnetic response of the bilayer by finding the angles θ_1 and θ_2 that minimize the total energy in Eq. (16). Elasticity affects these minimizing values of θ_1 and θ_2 because of the residual stresses generated by unequal magnetostriction of the layers as the magnetizations rotate. Elasticity has no effect on the remanent magnetization, as this is measured between fixed values of (θ_1,θ_2). However, elasticity can have a strong effect on the corner behavior and coercivity, as corners represent regions in which θ_1 and θ_2 change.

Figure 5 shows hysteresis loops for different values of λ_1 and λ_2 when the epitaxial strain $\epsilon^T = 0$, $Y_{\text{mod}} = 30\,000$, $\beta = 0.4$, $\alpha_1 = 0.15$, and $\alpha_2 = 0.3$. In the absence of elasticity ($\lambda_1 = \lambda_2 = 0$), this corresponds to Fig. 2(b) above. Also, because $\epsilon^T = 0$, results for (λ_1,λ_2) and $(-\lambda_1,-\lambda_2)$ are identical, as seen by Eq. (15).

We observe that elasticity changes the shape of the transitions and decreases the coercive field, i.e., narrows the hysteresis loop. The details depend strongly on the particular values of λ_1 and λ_2. When $\lambda_1 = 0.003$ and $\lambda_2 = 0.001$, elasticity has almost no effect on the coercivity and only a small effect on the transitions, while when $\lambda_1 = -0.001$ and $\lambda_2 = 0.003$, the coercive field decreases by about 25%.

The influence of elasticity is more apparent when $\alpha_1 = 0.3$ and $\alpha_2 = 0.15$. Figures 6(a) to 6(d) shows hysteresis loops in this case, for $\epsilon^T = 0$ and $Y_{\text{mod}} = 30\,000$ [Fig. 4(b) shows the results without elasticity]. As above, elasticity alters both transitions and the coercive field. When $\lambda_1 = 0.003$ and $\lambda_2 = 0.001$, elasticity smooths the corners but has negligible effect on the coercive field. When $\lambda_1 = 0.001$ and $\lambda_2 = 0.003$, elasticity increases the width of the corner loops and leads to a small (<20%) decrease in the coercive field. When $\lambda_1 = -0.003$ and $\lambda_2 = 0.001$, elasticity acts to close the corner loops and reduce the coercive field by close to 40%.

We next include epitaxial misfit ϵ^T. Because the misfit ϵ^T generates residual stress independent of magnetic field, it only affects the magnetic response in conjunction with

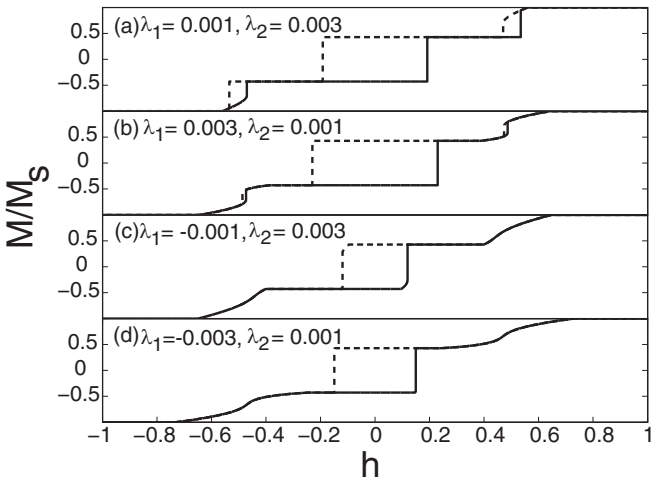

FIG. 6. Magnetic hysteresis curves are shown for different values of magnetostrictive strains λ_1 and λ_2, with epitaxial misfit $\epsilon^T = 0$ and thickness ratio $\beta = 0.4$. The magnetic anisotropies $\alpha_1 = 0.3$ and $\alpha_2 = 0.15$.

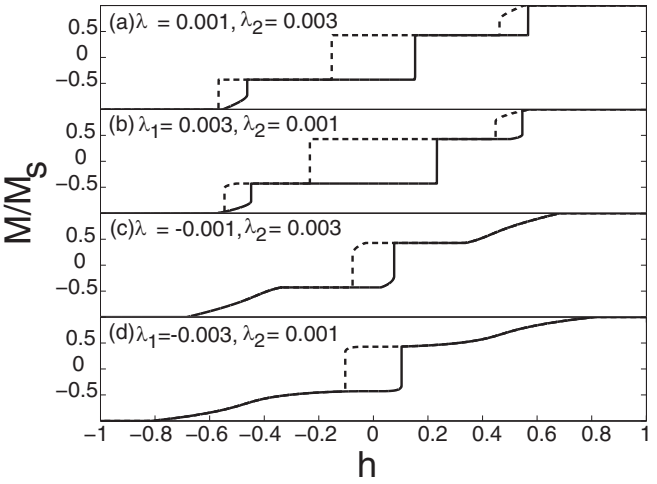

FIG. 8. Magnetic hysteresis curves are shown for different values of magnetostrictive strains λ_1 and λ_2, with epitaxial misfit $\epsilon^T = -0.002$ and thickness ratio $\beta = 0.4$. The magnetic anisotropies $\alpha_1 = 0.3$ and $\alpha_2 = 0.15$.

the magnetostrictive coefficients λ_1 and λ_2. Figure 7 shows hysteresis curves for different values of λ_1 and λ_2 when $\epsilon^T = 0.002$, while Fig. 8 shows the same curves when $\epsilon^T = -0.002$. In both figures, the magnetic anisotropies $\alpha_1 = 0.3$ and $\alpha_2 = 0.15$.

For the values of λ_1 and λ_2 shown, positive ϵ^T has less effect than negative ϵ^T. However, as results are identical for the triplets $(\lambda_1,\lambda_2,\epsilon^T)$ and $(-\lambda_1, -\lambda_2, -\epsilon^T)$ [see Eq. (15)], this reflects the relative signs of λ_1, λ_2, and ϵ^T rather than their absolute signs. For the combinations of λ_1, λ_2, and ϵ^T shown in Fig. 7, elasticity has little influence on the hysteresis curves. For example, when $\lambda_1 = 0.001$, $\lambda_2 = 0.003$, and $\epsilon^T = 0.002$, elasticity does not affect the magnetic hysteresis [compare Fig. 7(a) to Fig. 4(b)]. Interestingly, in this case adding the misfit actually decreases the elastic effect compared to the $\epsilon^T = 0$ case shown in Fig. 6(a). In fact, considering all the cases shown in Fig. 7, we observe that when $\epsilon^T = 0.002$, elasticity has a limited role in the shape of the transitions from the saturated states to the hysteresis loop, and has relatively little effect (<20%) on the coercive field.

In contrast, when we change the relative signs of λ_1, λ_2, and ϵ^T, as shown in Fig. 8, the role of elasticity on magnetic response is much more significant. When $\lambda_1 = 0.001$ and $\lambda_2 = 0.003$ [Fig. 8(a)], elasticity reduces the coercive field by about 30%, and also widens the corner loops. When $\lambda_1 = -0.001$ and $\lambda_2 = 0.003$ [Fig. 8(c)], elasticity decreases the coercive field by over 50% and closes the corner loops completely. There is a similar decrease in coercive field when $\lambda_1 = -0.003$ and $\lambda_2 = 0.001$ [Fig. 8(d)], where elasticity also forces a slow and smooth transition in the spin rotation angles away from the saturated states. We note that in the two cases shown in Figs. 8(c) and 8(d), if one increases the elastic energy by increasing Y_{mod}, the hysteresis loop continues to collapse, though the minimization algorithm fails before this occurs.

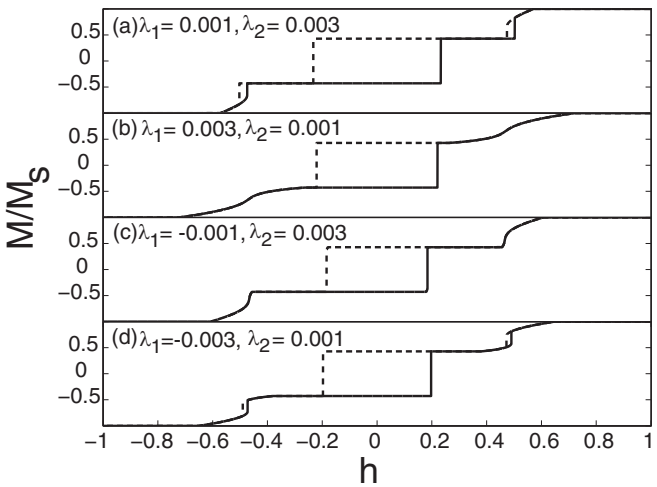

FIG. 7. Magnetic hysteresis curves are shown for different values of magnetostrictive strains λ_1 and λ_2, with epitaxial misfit $\epsilon^T = 0.002$ and thickness ratio $\beta = 0.4$. The magnetic anisotropies $\alpha_1 = 0.3$ and $\alpha_2 = 0.15$.

IV. DISCUSSION

Elastic energy owing to residual stresses in a magnetic bilayer can influence the magnetic response of the bilayer. We have shown that the elastic response impacts both the transitional behavior and the coercive field of the magnetic hysteresis loops of the bilayer. The transition regions are associated with changes in the magnetization angles θ_1 and θ_2, and so the addition of elastic energy to the magnetic energy changes the angles that minimize the total system energy. Because the energy is a complex function of the magnetization angles and the external magnetic field, even small changes to the energy can engender significant changes to values of θ_1 and θ_2 that minimize energy.

The main quantitative effect of elastic energy is on the coercive field. Figure 9 shows a plot of coercive field versus ϵ^T for the four different cases in the figures above: (a) $\lambda_1 = 0.001$, $\lambda_2 = -0.003$; (b) $\lambda_1 = 0.003$, $\lambda_2 = 0.001$; (c) $\lambda_1 = -0.001$,

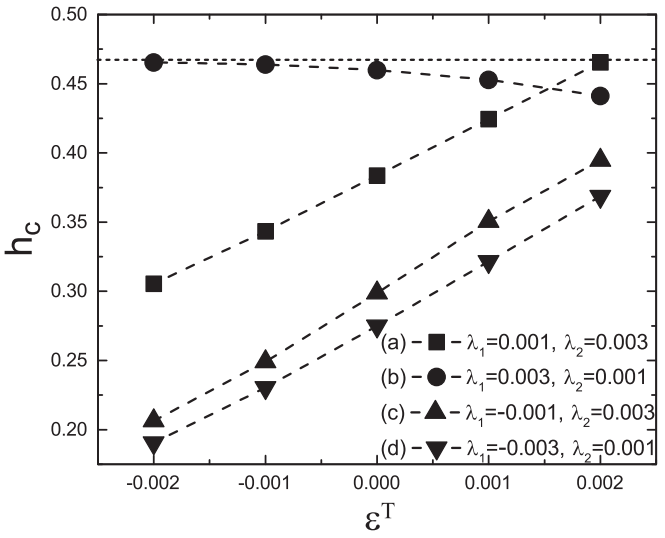

FIG. 9. Central loop coercive field h_c vs epitaxial strain ϵ^T for different magnetic expansion coefficients. The magnetic anisotropies $\alpha_1 = 0.3$ and $\alpha_2 = 0.15$.

$\lambda_2 = 0.003$; and (d) $\lambda_1 = -0.003$, $\lambda_2 = 0.001$. The horizontal line just above $h_c = 0.46$ gives the coercive field in the absence of elasticity. Elastic energy can decrease the coercive field by over a factor of two. In all the cases we have considered, we have not found any in which elasticity increases the coercive field.

Close examination of the elastic energy gives some insight as to how different elastic parameters led to different behaviors. Consider the elastic energy as a function of θ_1 when $\theta_2 = \pi$. We make this choice to see how the elastic energy affects the magnetic response as h increases from -1. In this case, the elastic energy is minimized either when $\theta_1 = 0$ (or π), or when $\theta_1 = \pi/2$. Recall that the elastic energy is independent of h because the constitutive equations (4) and (5) reflect that the magnetostrictive strain is proportional to the component of the magnetization in the direction of the easy axis.

When the elastic energy with $\theta_2 = \pi$ has a minimum at $\theta_1 = 0$ (or π) and a maximum at $\theta_1 = \pi/2$, it tends to lengthen the transition from the saturated state $(\theta_1,\theta_2) = (\pi,\pi)$ to the lower plateau of the hysteresis loop at $(\theta_1,\theta_2) = (0,\pi)$. However, the elastic energy has relatively little effect on the coercive field; that is, the magnetic field at which $(\theta_1,\theta_2) = (0,\pi)$ switches to the upper plateau of the hysteresis loop at $(\theta_1,\theta_2) = (\pi,0)$. In contrast, when the elastic energy with $\theta_2 = \pi$ has a maximum at $\theta_1 = 0,\pi$ and a minimum at $\theta_1 = \pi/2$, it tends to decrease the value of the coercive field at which $(\theta_1,\theta_2) = (0,\pi)$ switches to $(\theta_1,\theta_2) = (\pi,0)$. More, the decrease in the coercive field is tied to the depth of the minima at $\theta_1 = \pi/2$. In this case, it appears that the elastic energy helps nudge the system locally away from $(\theta_1,\theta_2) = (0,\pi)$ as h increases, even though it does not globally favor $(\theta_1,\theta_2) = (\pi,0)$. On decreasing h, the elastic energy has a similar role in pushing the system off the upper plateau at $(\theta_1,\theta_2) = (\pi,0)$.

The strength of the elastic effect depends in a complicated way on the magnitudes and signs of the elastic parameters. The values of the magnetic expansion coefficients λ_1 and λ_2 and the epitaxial strain ϵ^T have been chosen in order to look at a variety of cases, and with magnitudes consistent with linear elasticity. The normalized modulus $Y_{\rm mod}$ was chosen to be large enough so that there is an observable elastic effect on the magnetic hysteresis curves. Recalling that $Y_{\rm mod}$ is the ratio of the elastic modulus with the magnitude of the exchange coefficient between layers, we note that $Y_{\rm mod} = 30\,000$ is consistent with a modulus of 200 GPa (roughly that of iron) and an exchange coefficient of 6.7×10^6 J m^{-3}, as used by Hernandez *et al.* [23] (see Table I). For smaller $Y_{\rm mod}$, the exchange coupling between layers dominates the behavior, while for larger $Y_{\rm mod}$, elasticity becomes increasingly influential. We find that in some cases, increasing $Y_{\rm mod}$ beyond a certain critical value can cause the minimization algorithm to fail before the hysteresis loop is complete. Because of this, we have never seen complete collapse of the hysteresis loop.

Our analysis can be extended to systems with more than two layers. For example, the antiferromagnetic coupling we consider is often achieved by introducing nonmagnetic layers between ferromagnetic layers [5,6,11,12], so that the elasticity problem involves at least three layers. The presence of the nonmagnetic layer will affect not only the elastic energy, but also the magnitude of the coupling coefficient $j_{2:1}$ in Eq. (2). Specifically, since the magnitude of the coupling decreases as the distance between ferromagnetic layers increases [6,11], the influence of elasticity would increase, as $Y_{\rm mod}$ is normalized by $j_{2:1}$; see Eq. (16). We did not consider the role of the nonmagnetic layer in this paper, primarily because we wanted to gain some baseline understanding of the influence of magnetostrictive-driven elasticity on the magnetic properties of layered films.

V. CONCLUSION

An antiferromagnetically coupled bilayer composite media is studied by constructing the system's magnetic and elastic energies as functions of the applied magnetic field and the spin rotation angle of each layer. For a given set of magnetic and elastic parameters, the spin angles that minimize the normalized energy are found. These angles are used to construct the magnetic hysteresis loops of the system. In the absence of elastic energy, magnetic hysteresis loops depend on the magnetic anisotropies of the layers as well as the thickness ratio of the layers. Adding elasticity causes the layered system to stretch and bend when the spin rotation angles change, which is reflected in the spin transitions observed in the hysteresis curves as well as in the coercive field required to flip rotations as the magnetic field increases or decreases. The details of the elastic effect depend in a complicated way on the magnetostriction of the layers, the epitaxial strain between the layers, the magnetic anisotropies, and the system geometry.

ACKNOWLEDGMENT

The authors acknowledge the Department of Aerospace Engineering and Mechanics at University of Minnesota for supporting J.V.C. through a teaching assistantship.

[1] P. K. Amiri, Z. M. Zeng, J. Langer, H. Zhao, G. Rowlands, Y.-J. Chen, I. N. Krivorotov, J.-P. Wang, H. W. Jiang, J. A. Katine, Y. Huai, K. Galatsis, and K. L. Wang, Appl. Phys. Lett. **98**, 112507 (2011).

[2] Z. Zeng, G. Finocchio, and H. Jiang, Nanoscale **5**, 2219 (2013).

[3] D. Sander, Rep. Prog. Phys. **62**, 809 (1999).

[4] Michael Mezler, Denys Makarov, Alfredo Calvimontes, Daniil Karnaushenko, Stefan Baunack, Rainer Kaltofen, Yongfeng Mei, and Oliver G. Schmidt, Nano Lett. **11**, 2522 (2011).

[5] R. Lavrijsen, A. Fernández-Pacheco, D. Petit, R. Mansell, J. H. Lee, and R. P. Cowburn, Appl. Phys. Lett. **100**, 052411 (2012).

[6] C. W. Cheng, T. I. Cheng, C. H. Shiue, C. L. Weng, Y. C. Tsai, and G. Chern, IEEE Trans. Magn. **49**, 4433 (2013).

[7] Yuan-fu Chen, Yongfeng Mei, Rainer Kaltofen, Jens Ingolf Monch, Joachim Schummann, Jens Freudenberger, Hans-Jorg Klaub, and Oliver G. Schmidt, Adv. Mater. **20**, 3224 (2008).

[8] C. Barraud, C. Deranlot, P. Seneor, R. Mattana, B. Dlubak, S. Fusil, K. Bouzehouane, D. Deneuve, F. Petroff, and A. Fert, Appl. Phys. Lett. **96**, 072502 (2010).

[9] A. Kharmouche, S.-M. Chérif, A. Bourzami, A. Layadi, and G. Schmerber, J. Phys. D: Appl. Phys. **37**, 2583 (2004).

[10] W. Folkerts and S. T. Purcell, J. Magn. Magn. Mater. **111**, 306 (1992).

[11] P. J. H. Bloemen, H. W. van Kesteren, H. J. M. Swagten, and W. J. M. de Jonge, Phys. Rev. B **50**, 13505 (1994).

[12] R. W. Wang, D. L. Mills, Eric E. Fullerton, J. E. Mattson, and S. D. Bader, Phys. Rev. Lett. **72**, 920 (1994).

[13] W. X. Zhang, W. L. Zhang, B. Peng, H. C. Jiang, and S. Q. Yang, J. Magn. Magn. Mater. **278**, 9 (2004).

[14] J. Nogués and Ivan K Schuller, J. Magn. Magn. Mater. **192**, 203 (1999).

[15] T. Shima, H. Takahashi, K. Takanashi, and H. Fujimori, Sens. Act. A: Phys. **91**, 210 (2001).

[16] T. Shima, K. Takanashi, and H. Fujimori, J. Magn. Magn. Mater. **239**, 573 (2002).

[17] M. Sawicki, G. J. Bowden, P. A. J. deGroot, B. D. Rainford, J. M. L. Beaujour, R. C. C. Ward, and M. R. Wells, Phys. Rev. B **62**, 5817 (2000).

[18] Guohong Dai, Qingfeng Zhan, Yiwei Liu, Huali Yang, Xiaoshan Zhang, Bin Chen, and Run-Wei Li, Appl. Phys. Lett. **100**, 122407 (2012).

[19] Xiaoshan Zhang, Qingfeng Zhan, Guohong Dai, Yiwei Liu, Zhenghu Zuo, Huali Yang, Bin Chen, and Run-Wei Li, J. Appl. Phys. **113**, 17A901 (2013).

[20] N. A. Pertsev and H. Kohlstedt, Nanotechnology **21**, 475202 (2010).

[21] Ana L. Dantas, S. R. Vieira, and A. S. Carriço, Solid State Commun. **132**, 383 (2004).

[22] Zizheng Guo, Solid State Commun. **151**, 116 (2011).

[23] Stephanie Hernandez, Manish Kapoor, and R. H Victora, Appl. Phys. Lett. **90**, 132505 (2007).

[24] Roland Mattheis and Klaus Steenbeck, Phys. Eng. New Mater., Springer Proc. Phys. **127**, 151 (2009).

[25] H. J. Richter and A. Yu. Dobin, Appl. Phys. **99**, 08Q905 (2006).

[26] N. Tiercelin, V. Preobrazhensky, V. Mortet, A. Talbi, A. Soltani, K. Haenen, and P. Pernod, J. Magn. Magn. Mater. **321**, 1803 (2009).

[27] Victora Randall and H. Shen Xiao, Proc. IEEE **96**, 11 (2008).

[28] Zhihong Lu, P. B. Visscher, and W. H. Butler, IEEE Trans. Magn. **43**, 6 (2007).

[29] Haiwen Xi, Mark H. Kryder, and Robert M. White, Appl. Phys. Lett. **74**, 2687 (1999).

[30] Leonard Meirovitch, *Methods of Analytical Dynamics* (Dover, New York, 2003).

[31] Chun-Hway Hsueh, J. Appl. Phys. **91**, 9652 (2002).

[32] Ana L. Dantas, Selma R. Vieira, and A. S. Carrico, Phys. Rev. B **65**, 172414 (2002).

[33] B. D. Cullity and C. D. Graham, *Introduction to Magnetic Materials* (Wiley, Hoboken, NJ, 2009).

[34] Soshin Chikazumi, *Physics of Ferromagnetism* (Oxford University Press, Oxford, 1997).

[35] C. Tannous and J. Gieraltowski, Eur. J. Phys. **29**, 475 (2008).

[36] Martin H. Sadd, *Elasticity Theory, Applications and Numerics* (Elsevier, Oxford, 2005).

[37] Robert C. O'Handley, *Modern Magnetic Materials, Principles and Applications* (Wiley-Interscience, New York, 2000).

[38] Ohsung Song, Ph.D. thesis, MIT, 1994.

[39] Etienne du Trémolet de Lacheisserie, *Magnetostriction: Theory and Applications of Magnetoelasticity* (CRC, Boca Raton, FL, 1993).

[40] E. Tadmor and R. Miller, *Modeling Materials: Continuum, Atomistic and Multiscale Techniques* (Cambridge University Press, Cambridge, 2011).

[41] Eugene L. Allgower and Kurt Georg, *Classics in Applied Mathematics, Introduction to Numerical Continuation Methods* (SIAM, Philadelphia, PA, 2003).

[42] See Supplemental Material at http://link.aps.org/supplemental/10.1103/PhysRevB.94.054425 for details.

[43] B. Dieny, J. P. Gavigan, and J. P. Rebouillat, J. Phys: Condens. Matter **2**, 159 (1990).